Molecular Insights into n-Type Organic Thermoelectrics

CCS Chemistry

MINI REVIEW

Received: May 23, 2021 | Accepted: Aug. 7, 2021 | Published: Sept. 17, 2021

Molecular Insights into n-Type Organic Thermoelectrics

Shuyan Shao[1] & Jian Liu[2,3]*

[1]*Institute of Molecular Aggregation Science, Tianjin University, Tianjin 300072,* [2]*Zernike Institute of Advanced Materials, University of Groningen, 9747 AG Groningen,* [3]*Department of Chemistry and Chemical Engineering, Chalmers University of Technology, Göteborg 41296*

**Corresponding author: jian.liu@rug.nl; lijian@chalmers.se*

Cite this: *CCS Chem.* **2021**, *3*, 2702–2716

Organic thermoelectrics (OTEs) have been recently intensively investigated as they hold promise for flexible, large-area, and low-cost energy generation or heating–cooling devices for appealing applications, for example, wearable energy harvesting. In the past 7 years, n-type OTEs have witnessed a sharp increase in their performance thanks to significant progress in developing and understanding the fundamental physical properties of n-type OTE materials as well as the working principle and physical processes of the TE devices. In this mini review, we briefly review the advances and strategies of designing the n-type OTEs. More importantly, we discuss the effects of molecular structure of the n-type organic semiconductors on the fundamental physical processes such as charge transfer, separation, and transport, highlighting the key differences of the pristine and doped OTEs at the microscopic level. Finally, the remaining challenges and future outlooks of research are discussed. We aim to establish profound understanding of the structure–property–performance relationship to provide useful guidelines for the molecular design of high-performance n-type OTEs for promising future OTE technology.

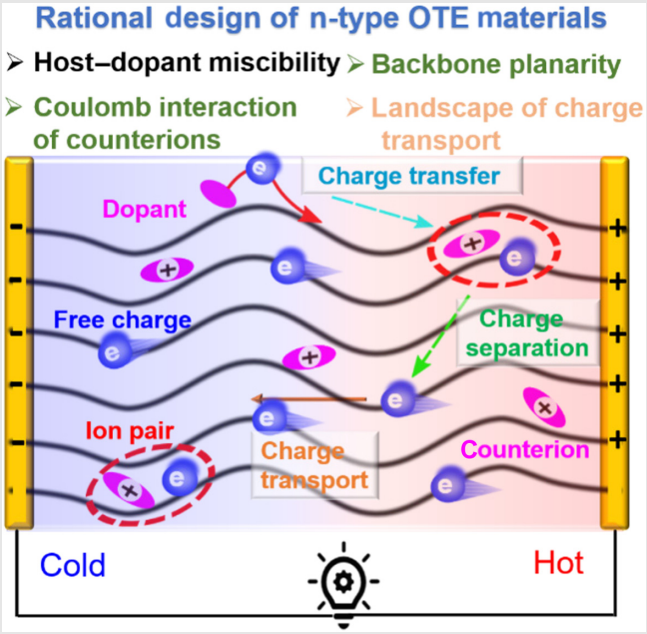

Keywords: **organic thermoelectrics, n-type organic semiconductors, molecular doping, side-chain engineering, backbone modification**

Introduction

Organic semiconductors (OSCs) have been widely used as the key functional material in a broad spectrum of applications including optoelectronics, energy storage, and biosensors due to natural advantages, such as low cost, mechanical flexibility, environmental or biocompatibility, and light weight.[1–8] Recently, there is emerging interest to apply OSCs to thermoelectrics (TEs),[9,10] potentially delivering flexible, large-area, and low-cost energy generation or heating–cooling devices for appealing applications, for example, wearable energy harvesting. The performance of TE materials is defined by the dimensionless figure of merit $zT = S^2\sigma T/\kappa$, where S, σ, and κ are the Seebeck coefficient, electrical conductivity, and thermal conductivity, respectively.[11] As the thermal

DOI: 10.31635/ccschem.021.202101167
Citation: *CCS Chem.* **2021**, 3, 2702–2716
Citation denotes calendar and volume year of first online publication.
Issue Assignment: Volume 3 (2021), Issue 10

conductivities of Van der Waals interacting OSCs are typically very low (κ < 0.5 Wm^{-1} K^{-1}),[12] power factor ($S^2\sigma$) is another important TE parameter for evaluating organic TE materials (OTEs). Early stage studies are mainly on p-type OTEs.[13–15] The record figure of merit of zT = 0.42 has been achieved by modulating the doping levels of poly(3,4-ethylenedioxythiophene):polystyrene sulfonate (PEDOT:PSS),[16] and a record high power factor of 2 mW m^{-1} K^{-2} has been reported for rubbed poly(2,5-bis (3-dodecyl-2-thienyl)thieno[3,2-b]thiophene) (PBTTT) films p-doped with the strong oxidant $FeCl_3$,[17] approaching those achieved in inorganic TE materials. The performance of p- and n-type TE materials should complement each other ahead of any practical applications such as constructing TE generators.[18] However, n-type OTEs are still far inferior to their p-type counterparts in terms of power factor and figure of merit.

Motivated by the unbalanced development of p- and n-type OTEs, the OTEs community has recently turned its focus to the more challenging n-type counterparts. Chabinyc and co-workers[19] reported a power factor of 0.1 μW m^{-1} K^{-2} for poly{[*N*,*N*′-bis(2-octyldodecyl)-naphthalene-1,4,5,8-bis(dicarboximide) (NDI)-2,6-diyl]-alt-5,5′-(2,2′-bithiophene)(BT)}(PNDI2OD-T2) doped by (4-(1,3-dimethyl-2,3-dihydro-1*H*-benzoimidazol-2-yl) phenyl)dimethylamine (*N*-DMBI). This example pioneers employing solution-processed conjugated polymer as an OTE. Afterward, a large variety of OSCs, including conjugated polymers and small molecules, have been utilized for n-type OTEs.[19–25] For example, Pei and co-workers[26] substituted the conjugated polymer backbone with halogen atoms to increase the electron mobility and electron affinity, leading to a high electrical conductivity of 14 S cm^{-1} and a power factor of 28 μW m^{-1} K^{-2}. Recently, they further modified the polymer structure by incorporating an extended and planar thiophene-fused benzodifurandione-based oligo(*p*-phenylenevinylene) (TBDOPV) backbone and achieved exceptional electrical conductivities as high as 90 S cm^{-1} and excellent n-type TE performances with power factors up to 106 μW m^{-1} K^{-2}, yielding a figure of merit of zT = 0.08.[27] Wang and Takimiya[28] reported an acceptor (A)–acceptor n-type copolymer consisting of naphthodithiophenediimide and bithiophene imide building blocks showing an impressive n-type conductivity value of up to 11.6 S cm^{-1} and power factor up to 53.4 μW m^{-1} K^{-2}. Huang et al.[29] reported small molecule hosts, dihydropyrrolo[3,4-c]pyrrole-1,4-diylidenebis(thieno[3,2-b]thiophene) derivatives, with aromatic structures. They achieved a maximum power factor and zT values of up to 236 μW m^{-1} K^{-2} and 0.26 using *N*-DMBI as the n-type dopant. Very recently, Koster and co-workers[30] demonstrated a record high figure of merit of zT = 0.34 by molecularly n-doping a fullerene derivative with meticulous design of the side chain.

Looking back on the history of n-type solution-processed OTEs, the TE performance has been mainly boosted by designing new structures of host or dopant molecules.[31–33] Much of the conventional wisdom of molecular design of n-type OTE materials derives from the knowledge of the structure–performance relationship of intrinsic OSC films applied in optoelectronic devices, that is, photovoltaics and field-effect transistors. While OTEs exploit the properties of the doped OSC films, which involves the complex electronic interactions between the host and the dopant materials, most previous experience and knowledge inherited from other divisions of organic electronics cannot be simply applied to OTEs. Recent studies have gained deeper understanding of the working principle of the TE devices by investigating the fundamental properties of the host and dopant materials as well as the interactions and physical processes between them at the microscopic level. Many new insights into the molecular design of n-type OTEs have been gradually accumulated by the OTE community. These fundamental advancements have spurred the recent fast development of n-type OTE materials. Although there are many nice review papers on organic TEs, only a few of them are specifically on the n-type counterpart, which mainly focus on the development of different types of materials such as small molecules, conjugated polymers, or composite materials rather than the underlying physical insights.[20,34–36]

In this mini review paper, we overview the emerging insights into the structure–property–performance relationships and the advances of n-type OTE materials. We first briefly discuss the elementary steps of TE processes within n-type OTE materials. Then we illustrate how the emerging insights, including host–dopant miscibility, backbone planarity, electrostatic interaction control by counterions, and energetic and spatial landscape of charge transport tailoring, catalyzed the recent development of n-type OTE materials. We emphasize the unique insights of molecular design of OTE materials from those for other optoelectronic applications based on the properties of pristine OSCs. Finally, the remaining challenges and an outlook of future research are discussed.

Elementary Processes of TE Transport

From the definition of the figure of merit given in the introduction, electrical conductivity σ and Seebeck coefficient *S* are two important parameters to be optimized, and they are defined by the following equations

$$\sigma = \mu \cdot n \cdot q \tag{1}$$

$$S = \frac{k_B}{e} \int \frac{(E_F - E)}{kT} \times \frac{\sigma(E)}{\sigma} dE \tag{2}$$

DOI: 10.31635/ccschem.021.202101167
Citation: *CCS Chem.* **2021**, 3, 2702–2716
Citation denotes calendar and volume year of first online publication.
Issue Assignment: Volume 3 (2021), Issue 10

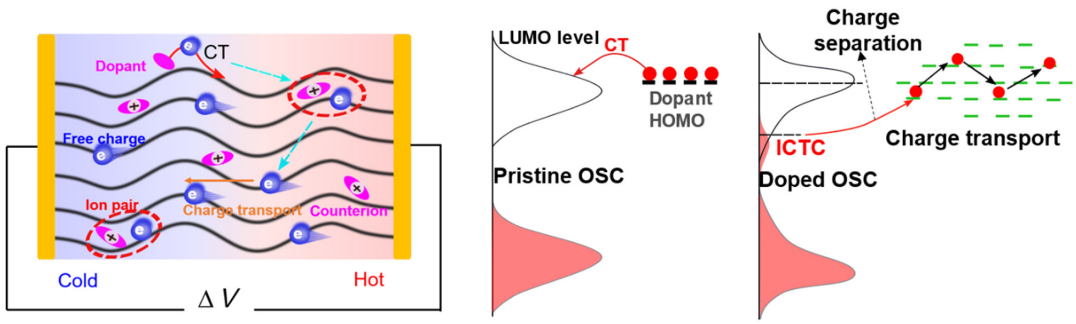

Figure 1 | *The thermoelectric transport process of n-type molecularly doped OSCs.*

where μ, n, k_B, and E_F are charge mobility, free charge density, the Boltzmann constant, and fermi energy level, respectively; σ(E) is the energy-dependent electrical conductivity, including a term describing density of states (DOS) distribution, and $\sigma = \int \sigma(E) dE$ is the total electrical conductivity. Both σ and S are the function of charge carrier density and trade off with each other. The elementary TE steps behind these formulas include charge transfer between the host and dopant molecules, charge separation of integer charge-transfer complexes (ICTC), and entropy-carrying charge transport (Figure 1), which are all related to the charge carrier. The TE transport is characterized not only by the charge mobility but also by the energetic position of charge carriers relative to the Fermi level. To design high-performance n-type OTEs, one must take each elementary step of the TE process into account. The following sections will discuss different aspects regarding rational molecular design of n-type TE materials.

Insights into Molecular Design of n-Type OTEs

Host–dopant miscibility

Molecular doping is a powerful strategy to modulate the charge carrier density, which typically involves redox reaction between the host and dopant molecules.[37–39] It means that the two types of molecules should be in proximity to enable an effective charge transfer, where the transferred charge is either full or partial. The doping efficiency is defined by the ratio of free charge density to the number of introduced dopant molecules. For most n-type OTE materials, mixed films of host and dopant molecules are deposited by solution co-processing. The intimate contact between host and dopant molecules highly depends on the interaction and mixing entropy. Large phase separation occurs if there is a big difference in polarity between host and dopant molecules or a high doping concentration. For example, Chabinyc and co-workers[19] observed many dopant aggregates on the surface of the thin film and a low doping efficiency of approximately 1% when solution co-processing of non-polar donor (D)–A polymer PNDI2OD-T2 with polar *N*-DMBI dopant was performed. The large number of dopant aggregates greatly reduces the interfacial area between the host and dopant molecules, limiting the charge-transfer efficiency and the eventual doping efficiency.

Matching the polarity between the host and dopant materials is one effective way to overcome the issue of phase segregation. Liu et al.[24] employed a polar triethylene glycol-type side chain to enhance polarity of a fullerene derivative (PTEG-1), which improved the miscibility between the polar host and polar dopant molecules (Figure 2a). Thus, the doping efficiency between PTEG-1 and *N*-DMBI reached a value of approximately18% with an optimized electrical conductivity of 2.05 S cm^{-1}, leading to a power factor of 16.7 μW m^{-1} K^{-2} at 40 mol % doping concentration. The strategy of incorporating polar side chains has been further extended to conjugated polymers based on the NDI-BT backbone and n-type dopant (Figure 2b).[20,41–43] Coarse-grained molecular dynamics simulations found that the free energy of transfer required to move an *N*-DMBI molecule from the alkyl to the TEG phase is –16 kJ mol^{-1}, quantifying further the strong preference of the dopant for the TEG phase over the alkyl one (Figure 2c). n-Type dopant molecules were experimentally evidenced to reside within the phase of polar side chains rather than the hydrophobic alkyl side chains, which explains the improved host–dopant miscibility at a nanoscale level. Consequently, an increased doping efficiency of >10% and higher power factor of 0.4 μW m^{-1} K^{-2} were obtained when using *N*-DMBI as the dopant.

Another effective way to increase the host–dopant miscibility is by tailoring the conformation or the packing motif of conjugated polymer chains. Perry et al.[44] reported that, by doping an ambipolar D–A polymer with the nonplanar donor poly((*E*)-3-(5-([8,8′-biindeno [2,1-*b*] thiophenyli- dene]-2-yl)thiophen-2-yl)-2,5-bis(*n*-icosyl)-6(thiophen-2-yl)- pyrrolo[3,4-c]pyrrole-1,4(2*H*,5*H*)-dione) [P(BTP-DPP)] through a sequential procedure, a high electrical conductivity of 0.45 S cm^{-1} was achieved, which is five orders of magnitude higher than the reference

DOI: 10.31635/ccschem.021.202101167
Citation: *CCS Chem.* **2021**, 3, 2702–2716
Citation denotes calendar and volume year of first online publication.
Issue Assignment: Volume 3 (2021), Issue 10

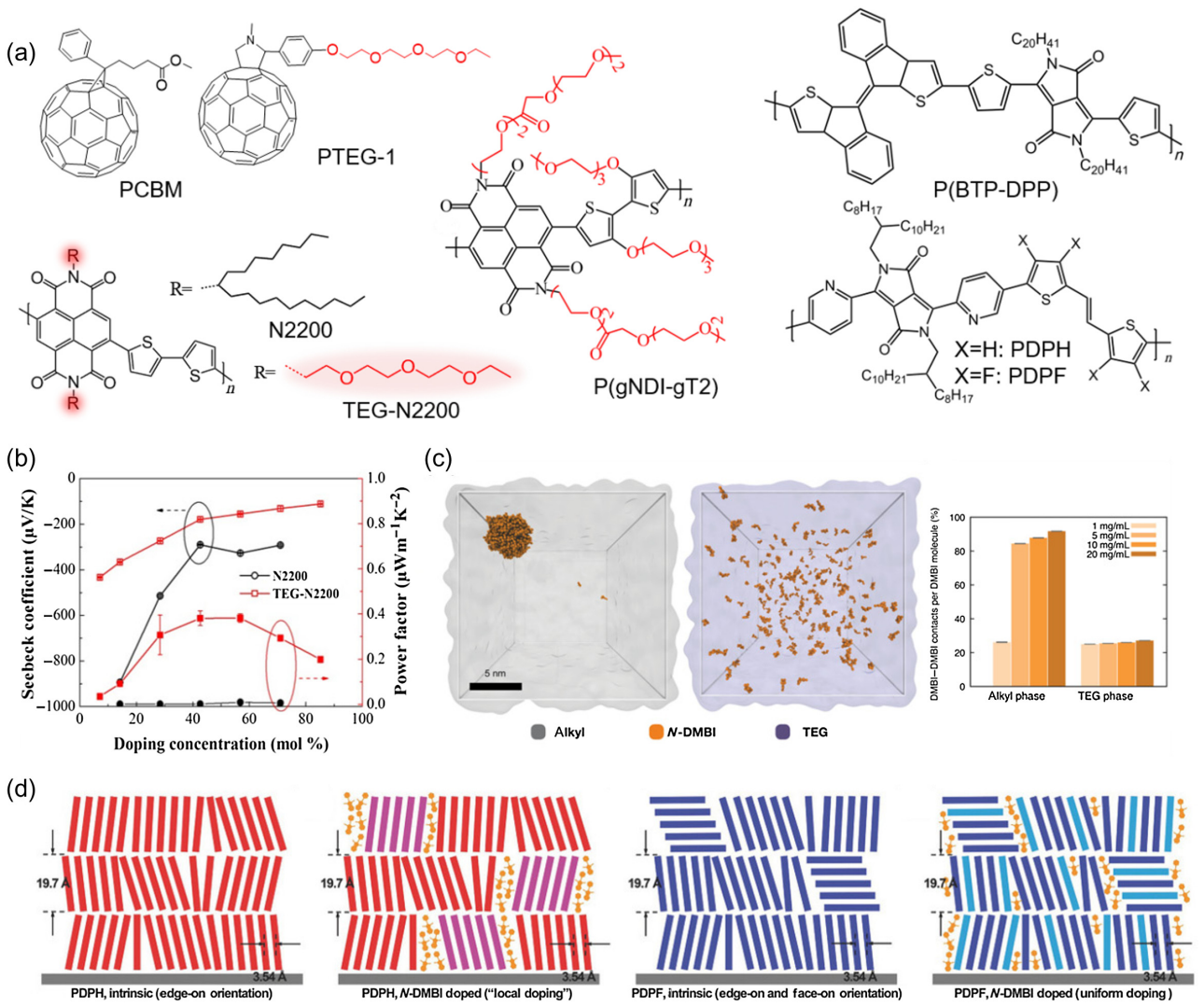

Figure 2 | *(a) Chemical structures of fullerene derivatives and conjugated polymers. (b) Seebeck coefficient and power factor of N2200 and TEG-N2200 as a function of doping concentration. (c) Molecular dynamic simulations of polar dopant in different matrixes. (d) The schematic of molecular packing of doped PDPH and PDPF films. Reprinted with permission from the ref 20. Copyright 2018 Wiley-VCH, and the ref 40. Copyright 2018 Wiley-VCH.*

P(NDI2OD-T2) sample. The space created by the nonplanar donor consistuents in the backbone can improve its miscibility with the extrinsic dopant molecules. Likewise, Sommer and co-workers[45] demonstrated an improved host–dopant miscibility by using an NDI-2T copolymer incorporating "kinked" monomers. In contrast, it was reported that a mixture of edge- and face-on orientations could create free space at boundaries, allowing for a better accommodation of dopant molecules in the matrix of conjugated polymers.[40,46] This enables an improved host–dopant miscibility, and, thus, a higher doping efficiency and TE performance, as compared with either one of the oriented configurations (Figure 2d). Regardless of nonplanar backbone or mixed orientations, the principle of these strategies is to create free space for accommodating dopant molecules to improve the miscibility and increase the doping efficiency. However, these strategies sacrifice charge transport: the former strategy degrades the intramolecular charge transport, whereas the latter may compromise the charge transport pathway.

Backbone planarity

Backbone planarity is an important factor that dictates the conformation of polymer chains in solution or solid states.[27,47,48] However, most of the highest electron field-effect mobilities have been achieved in n-type D–A conjugated polymers.[49–53] This implies that the backbone planarity of D–A copolymers are sufficient to provide excellent intrachain charge transport in the undoped state. Highest occupied molecular orbital (HOMO) and

DOI: 10.31635/ccschem.021.202101167
Citation: *CCS Chem.* **2021**, 3, 2702–2716
Citation denotes calendar and volume year of first online publication.
Issue Assignment: Volume 3 (2021), Issue 10

lowest unoccupied molecular orbital (LUMO) coefficients of a D–A conjugated polymer are localized on the D and A moieties, respectively.[54,55] In a theoretic study, Fazzi et al.[56] demonstrated that the negative charge of the benchmark D–A copolymer P(NDI2OD-T2) induces the relaxation mainly on NDI moieties and affects the torsional angle between D and A moieties, leading to charge localization within a single polymer chain. Naab et al.[48] have investigated a series of n-type conjugated polymers with various backbone structures in terms of field-effect mobility of the pristine state and electrical conductivity of the doped state. A highest conductivity of 0.45 S cm^{-1} was achieved for the ethynylene-linked conjugated copolymer that has the smallest D–A character among various conjugated polymers.[48] In a similar sense, Lu et al.[27] reported a series of conjugated polymers incorporating thiophene-fused benzodifurandione-based oligo(*p*-phenylenevinylene) (TBDOPV) as the main building unit, which is linked by an ethylene, thienylene, or bithiophene bridging unit, respectively. Although the three copolymers exhibit similar field-effect charge mobilities, the one with an ethylene linker has the most planar backbone and the best electrical conductivity of 90 S cm^{-1} and power factor of 106 μW m^{-1} K^{-2} (see the chemical structures in Figure 3a). These studies reveal that the electrical conductivity of a doped film does not correlate with the field-effect electron mobility measured for the pristine state, and conjugated polymers used for n-doping applications should be designed to have long polaron delocalization length in the charged state, which is dictated by the excellent backbone planarity.

Wang et al.[22] doped a ladder-type semiconductive polymer, named solution-processible n-type polybenzimidazobenzophen-anthroline (BBL), with strong reducing agents such as tetrakis(dimethylamino)ethylene (TDAE), and the benchmark polymer P(NDI2OD-T2) was used as the reference. The density functional theory (DFT) computed polaron delocalization length for the linear "torsion-free" homopolymer BBL is larger than that of the distorted D–A copolymer P(NDI2OD-T2), suggesting an easier intramolecular transfer, thus, a higher polaron mobility along the chain for the ladder-type polymer (Figure 3b). Therefore, n-type conductivity as high as 2.4 S cm^{-1} and a power factor of 0.43 μW m^{-1} K^{-2} were achieved for the doped BBL,[22] representing three orders of magnitude higher than those measured for the reference polymer (Figure 3c). This study established a simple picture that clarifies the correlation between the degree

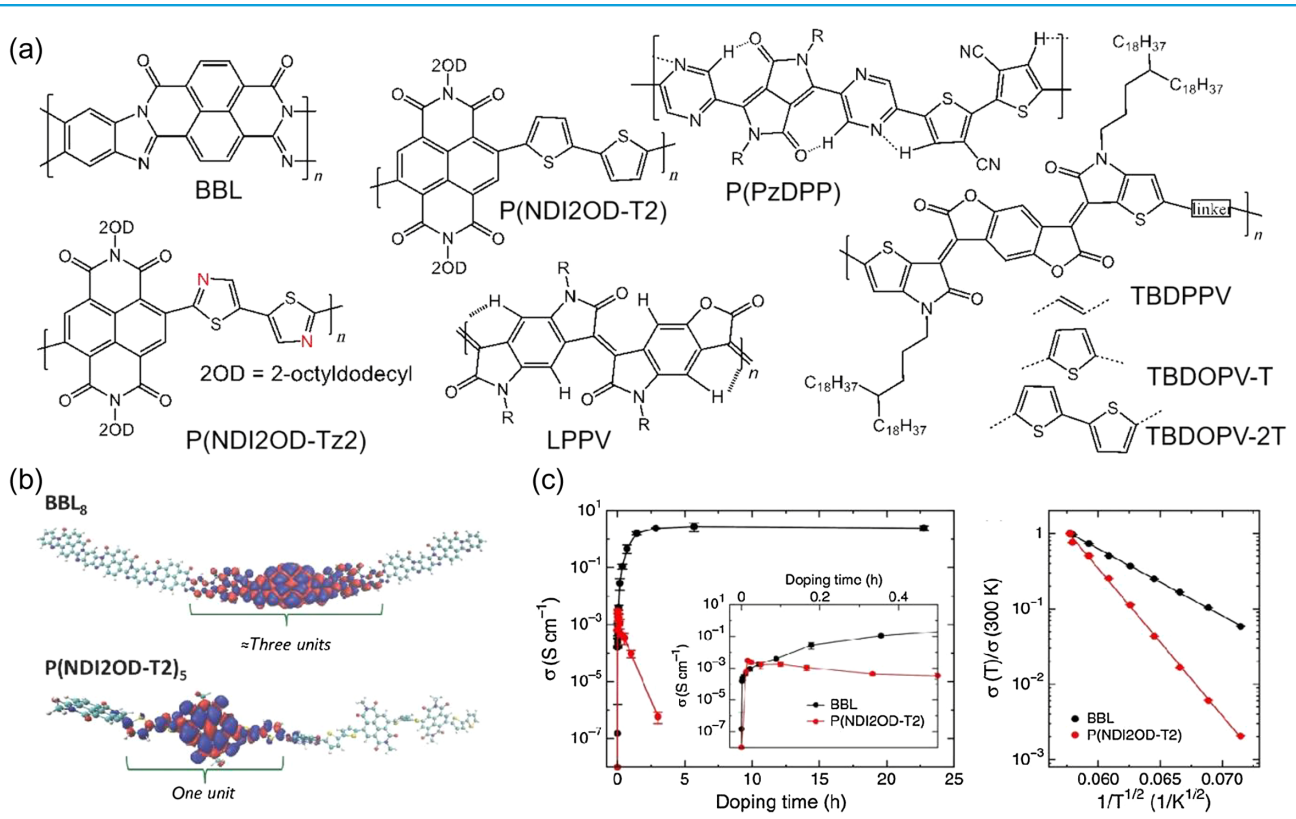

Figure 3 | *(a) Chemical structures of D–A and A–A conjugated copolymers. (b) Spin (α and β) density distributions of the longest BBL (n = 8, top) and P(NDI2OD-T2) (n = 5, bottom) oligomers, as obtained with the BS-UDFT and UDFT calculations, respectively, at the (ωB97X-D3/6-31G)* level. (c) Temperature-dependent electrical conductivity of doped BBL and P(NDI2OD-T2) films. Reprinted with permission from the ref 57. Copyright 2016 Wiley-VCH.*

DOI: 10.31635/ccschem.021.202101167
Citation: *CCS Chem.* **2021**, 3, 2702–2716
Citation denotes calendar and volume year of first online publication.
Issue Assignment: Volume 3 (2021), Issue 10

of backbone planarity and the polaron delocalization length. The same group further extended the same concept into NDI-based conjugated polymer, and designed a new n-type conjugated polymer by replacing the D moiety bithiophene with bithiazole.[57] The reduced intrachain steric demands in Tz2 versus T2 give rise to greater backbone planarity, hence stronger intermolecular π–π stacking interactions. Furthermore, the electron-deficient nature of Tz2 enhanced the electron affinity and reduced the D–A character. This backbone modification caused a negligible change in field-effect electron mobility. However, upon doping, P(NDI2OD-Tz2) reached an electrical conductivity of ≈0.1 S cm^{-1} and power factor of 1.5 μW m^{-1} K^{-2}. Pei and co-workers[58] reported two rigid coplanar poly(*p*-phenylene vinylene) (PPV) derivatives, LPPV-1 and LPPV-2 with nearly torsion-free backbones because the intramolecular hydrogen bonds formed between the hydrogen atoms and the carbonyl groups lock the conformation. The fused electron-deficient rigid structures endow the derivatives with less conformational disorder and low-lying LUMO levels of −4.49 eV. Upon doping, two conjugated polymers exhibited a high n-doping efficiency and significantly improved air stability, leading to a high electrical conductivity of up to 1.1 S cm^{-1} and a power factor as high as 1.96 μW m^{-1} K^{-2}. Yan et al.[59] extended the conformation lock strategy to a new diketopyrrolopyrrole (DPP) derivative, pyrazine-flanked DPP (PzDPP), leading to a planar D–A backbone structure, the deepest LUMO level in all the reported DPP derivatives, and strong interchain interaction with a short π–π stacking distance of 3.38 Å. When doped with n-dopant *N*-DMBI, this DPP-based conjugated polymer exhibited high n-type electrical conductivities of up to 8.4 S cm^{-1} and power factors of up to 57.3 μW m^{-1} K^{-2}.

The important insight gained by previous studies is that the backbone planarity is more significant for improving TE performance than for realizing high field-effect mobility. A large degree of backbone planarity enables not only an increased electron affinity for maximizing the doping level but also a high tolerance to the doping process. Any undesired backbone relaxations upon charging could be mitigated by increasing the degree of backbone planarity, leading to more extended polaron delocalization along the intrachain direction. In short, the large backbone planarity is beneficial for increasing both charge carrier density and bulk charge mobility, thus leading to a higher electrical conductivity and power factor.

Controlling the electrostatics of counterions

Molecular doping of the organic materials normally occurs in two steps.[60] First, complete or partial charge transfer between host and dopant molecules occurs, forming coulombically bounded charge and counterion pairs. In the secondary step, the charge-ion pairs dissociate into free charges through thermal ionization. In most cases, OSCs have low dielectric constants ($\varepsilon_r \approx 3$),[61] which lead to high binding energy on the order of several hundred meV.[62,63] There is a growing interest in exploring the Coulomb interaction for molecular doping and OTEs. Aubry et al.[64,65] demonstrated that the Coulomb interaction in doped polythiophene films could be screened using bulky dodecaborane clusters as the p-type dopant, leading to a high bulk hole mobility and electrical conductivity.

Liu et al.[66] explored the impact of electrostatic interaction on the doping efficiency in lightly n-doped fullerene derivatives with different dielectric constants ([6,6]-phenyl-C61-butyric acid methyl ester (PCBM) with $\varepsilon_r \approx 3.7$ and PTEG-1 with $\varepsilon_r \approx 5.9$). It was found that the doping efficiency of lightly doped PCBM layers was only a few percent, but doped PTEG-1 films exhibited a very high doping efficiency approaching 100%. They attributed the high doping efficiency of doped PTEG-1 to the stabilizing electrostatic interaction between charge-ion pairs and the polar side chain of PTEG-1. For most doped organic films, the electrical conductivity often reaches a peak value at a certain doping concentration, beyond which it decreases quickly. Recently, Koopmans et al.[67] combined analytical work and Monte Carlo simulations to demonstrate that carrier–carrier interactions can cause this conductivity decrease and reduce the maximum conductivity by orders of magnitude, possibly in a broad range of materials. The simulation results indicate that the Coulomb interaction from the counterions can decrease the electrical conductivity but barely influence the trend of electrical conductivity versus the doping concentration. In addition, they also argued that a higher dielectric constant or large delocalization length of charge carriers are beneficial for reducing the negative effects of charge–charge interaction, leading to a higher electrical conductivity.

Koster and co-workers[47] performed a comparison study on vapor doping two n-type conjugated polymers (benchmark D–A copolymer N2200 versus A–A poly (2,2′-bithiazolothienyl-4,4′,10,10′-tetracarboxydiimide PDTzTI) for thermoelectrics. Doped N2200 film rendered an inefficient free charge generation, poor charge transport, and a very low power factor of 0.06 μW m^{-1} K^{-2}. In contrast, doped PDTzTI demonstrated huge enhancements in terms of free charge generation and transport, leading to a remarkable conductivity of 4.6 S cm^{-1}, power factor of 7.6 μW m^{-1} K^{-2}, and zT of 0.01 at room temperature. This study indicates that enhanced molecular planarity and packing density of conjugated polymer together with a reduced D–A character promote two-dimensional charge delocalization, and facilitate charges escaping from the Coulomb interaction. As such, the charge-ion pairs are more easily dissociated into free charges. Very recently, the same group reported a D–A

DOI: 10.31635/ccschem.021.202101167
Citation: *CCS Chem.* **2021**, 3, 2702–2716
Citation denotes calendar and volume year of first online publication.
Issue Assignment: Volume 3 (2021), Issue 10

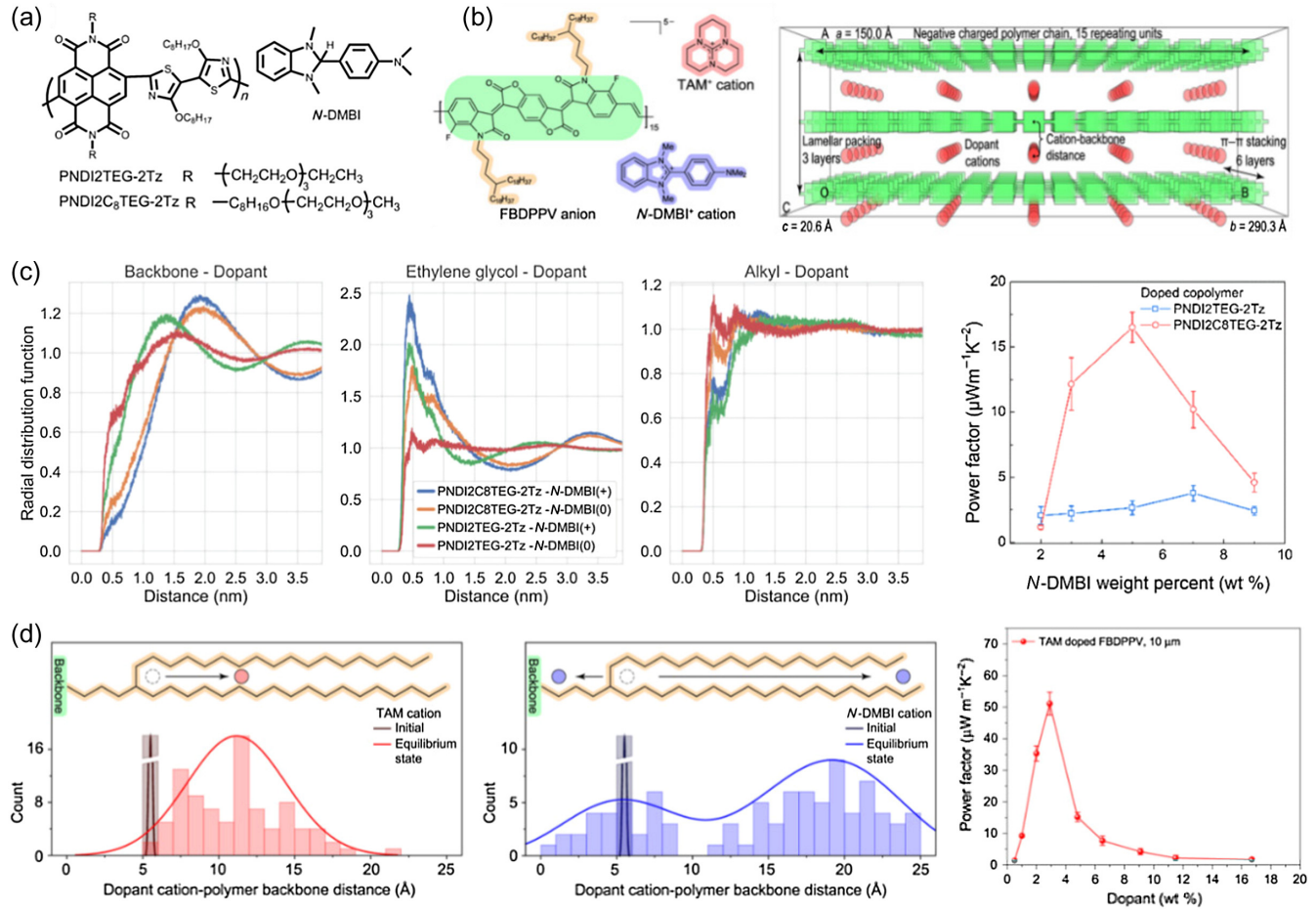

Figure 4 | *(a) The chemical structures of NDI-2Tz-based conjugated polymers with polar and amphipathic side chains. (b) Chemical structures of FBDPPV anions, TAM⁺, and* N*-DMBI⁺ cations. Schematic diagram of initial supercell for molecular dynamics which contains FBDPPV anions and TAM⁺ (or* N*-DMBI⁺) cations. Polymer alkyl chains are hidden for clarity. (c) Dynamic molecular simulation and power factor as a function of doping concentration for doped NDI-2Tz-based conjugated polymers with polar and amphipathic side chains. (d)* N*-DMBI-doped FBDPPV. Light green represents the FBDPPV backbone, orange represents the FBDPPV alkyl side chain, and red-blue represents the dopant cation. TAM⁺ cation has distinctly weaker interactions with polymer backbones, whereas* N*-DMBI⁺ cation presents stronger interactions with polymer backbones, the plot of power factor as a function of doping concentration. Reprinted with permission from the ref 68. Copyright 2021 Wiley-VCH, and the ref 69. Copyright 2020 Springer Nature.*

copolymer featuring amphipathic side chains (PNDI2C8-TEG-2Tz) (Figure 4a). Distinct from conjugated copolymers with mere alkyl side chains or ethylene glycol-type side chains on A moieties,[20,40,70] the conjugated copolymer with amphipathic side chains contains an alkyl chain segment as a spacer between the backbone and ethylene glycol-type chain segment. An electrical conductivity of 1.6 S cm^{-1} and a power factor of 16.5 ± 1.2 μW m^{-1} K^{-2} have been achieved for the doped copolymer with amphipathic side chains, representing an fivefold increase as compared with the reference polymer with polar side chains (Figure 4c).[68] The alkyl spacer not only reduces the energetic disorder of the conjugated polymer film but also properly controls the spatial location of the dopant molecules away from the backbone, which minimizes the adverse influence of counterions.

Very recently, Pei and co-workers[69] have reported a computer-assisted screening approach to rationally design a triaminomethane-type dopant (TAM), which exhibits extremely high stability and a strong hydride donating property due to its thermally activated doping mechanism (Figure 4b). More importantly, as compared with conventional n-type dopant *N*-DMBI, TAM negligibly perturbs the polymer backbone conformation and microstructural ordering. After ionization, TAM cations possess weak π-backbone affinity but strong intrinsic affinity with side chains, which enables the doped system to screen the Coulomb potential.[71] Such doping features lead to high probability of free charge generation for TAM-doped polymers and further result in an excellent conductivity of up to 22 ± 2.5 S cm^{-1} and a power factor of over 80 μW m^{-1} K^{-2},

DOI: 10.31635/ccschem.021.202101167
Citation: *CCS Chem.* **2021**, 3, 2702–2716
Citation denotes calendar and volume year of first online publication.
Issue Assignment: Volume 3 (2021), Issue 10

which are significantly higher than those values achieved by using the common n-dopant *N*-DMBI (Figure 4d).

The n-type OTE studies exploring the Coulombic effect have the common goal to precisely control the dopant (or dopant cation) location relative to conjugated backbones. As is well known, the molecular doping of OSCs is usually carried out by mixing the host and dopant molecules, posing a great challenge in controlling the dopant location. An interesting insight gained from previous work is that the one should maximize the affinity of the dopant with the side chains over that with the backbone. It enables a favorable nanostructure, within which the dopant molecules mainly reside in the side chain phase rather than within the π-stacking of the backbone. The mitigated Coulomb interaction enables not only a higher doping efficiency but also an improved bulk mobility. Importantly, it also provides a pathway to overcoming the trade-off between the electrical conductivity and the Seebeck coefficient, leading to a higher power factor.

Energetic and spatial landscape of charge transport

DOS distribution

For most OSCs with disordered nature, the charge transport occurs by charge carrier hopping over an energetic landscape, which is characterized by Gaussian-shaped DOS distribution,[72,73]

$$g(E) = \frac{N_m}{\sqrt{2\pi}\sigma_d} \exp\left[-\left(\frac{E-E_{ct}}{\sqrt{2}\sigma_d}\right)^2\right] \quad (3)$$

where N_m is the total concentration of localized states, σ_d is the Gaussian DOS width, and E_{ct} is the energy of the state. The charge carriers generated by the molecular doping fill the DOS, lifting the E_F up toward the E_T. Alternatively, eq 2 can be rewritten in terms of the E_T as

$$S = -\frac{1}{qT}(E_T - E_F), \quad (4)$$

where the transport energy is defined as

$$E_T = \int E \frac{\sigma(E)}{\sigma} dE. \quad (5)$$

Besides the charge generation, the molecular doping can impact the shape of DOS as well. Several theoretical studies point out that the Coulomb interaction from counterions are likely to broaden the DOS and act as Coulomb traps to reduce the carrier mobility.[74,75] Doped OSCs typically exhibit a thermal activation of their electrical conductivity. Schwarze et al.[76] explored the molecular origin for the thermal activated transport in a wide range of doped organic films. Their study indicates that the Arrhenius activation energy of charge transport is largely determined by the Coulomb interaction of counterions for a given doping level when the doping concentration is below 10 mol %. At very high doping concentration (>10 mol %), the activation energy gradually saturates, and mainly depends on the static energetic disorder and reorganization energy of doped materials. This point implies that the activation energy might be an easily accessible parameter for estimating energetic disorder of highly doped OSCs. As implied by eq 4, the sign of the Seebeck coefficient is determined by the relative positions of the E_F and E_T. When a Gaussian DOS is filled such that the E_F sits below the center of the DOS for n-doped OSCs, the Seebeck coefficient is typically negative, whereas it should be positive for p-doped films with E_F sitting above the center of the DOS. From this point of view, the sign of the Seebeck coefficient is usually used to confirm the type of the majority charge carriers by the community. Clearly, both electrical conductivity and Seebeck coefficient are not only influenced by the charge carrier density but also determined by the shape of the DOS.

It is highly desired to enhance the TE performance by tailoring the DOS in the TE field. Mahan and Sofo[77] theoretically proposed the concept of a delta-shaped transport distribution, situated somewhere above the Fermi energy, to maximize the TE properties. Later Katz et al.[78] experimentally proved this idea of DOS engineering in 2,3,5,6-tetrafluoro-7,7,8,8-tetracyanoquinodimethane (F4TCNQ)-doped poly(3-hexylthiophene) (P3HT) by blending in a small fraction of poly(3-hexylthiophene)-thiophene, thereby increasing *S* from approximately 580 to 700 μV/K while preserving electrical conductivity. Kemerink and co-workers[79] have recently revisited the strategy of DOS engineering proposed by Mahan and Sofa, and achieved a very high Seebeck coefficient of >1 mV K^{-1} by mixing two p-type conjugated polymers with an energetic offset as the host. These studies fall in the category of p-type OTEs while reports on tailoring the DOS of n-type OTEs are scare in the literature.

A recent study by Liu et al.[25] demonstrated how to increase the n-type organic TE performance by tailoring the DOS with introduction of sp^2-nitrogen (N) into the D moiety of an NDI-2T backbone (Figure 5a). Such a backbone modification improves not only the molecular planarity but also the structural order. Interestingly, they observed an unusual sign switching of the Seebeck coefficient from negative to positive by just increasing the dopant loading in the D–A copolymer without sp^2-N atoms. They directly measured the DOS distribution profiles of pristine and doped conjugated polymers by an electrochemical method based on ionic liquid electrolyte. The results indicate that the DOS distributions become narrower after backbone modification in both the

DOI: 10.31635/ccschem.021.202101167
Citation: *CCS Chem.* **2021**, 3, 2702–2716
Citation denotes calendar and volume year of first online publication.
Issue Assignment: Volume 3 (2021), Issue 10

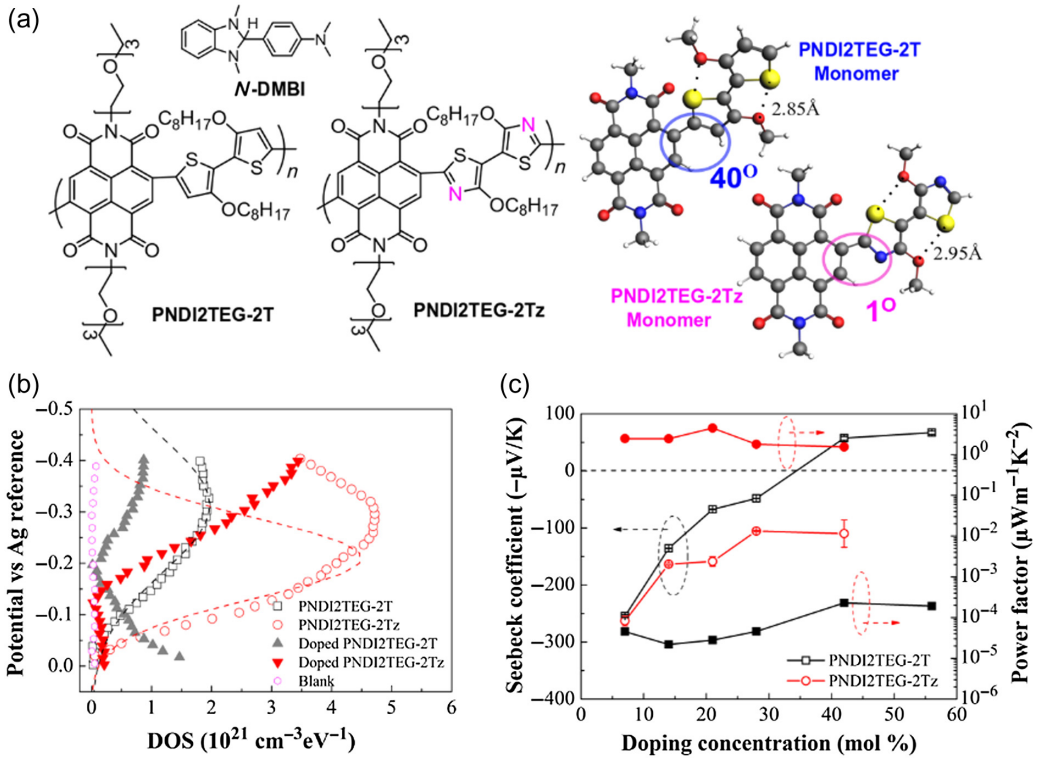

Figure 5 | *(a) Chemical structures of PNDI2TEG-2T and PNDI2TEG-2Tz, and DFT-optimized geometries for PNDI2-TEG-2T repeat unit and PNDI2TEG-2Tz repeat unit. Alkyl and* N*-ethylene glycol substituents are replaced by methyl groups to simplify the calculations. (b) The measured DOS functions of PNDI2TEG-2T and PNDI2TEG-2Tz in the pristine (open symbols) and 28 mol %-doped state (closed symbols). The dashed lines are Gaussian fits. (c) The plots of the Seebeck coefficient and power factor as a function of doping concentration. Reprinted with permission from the ref 25. Copyright 2018 Wiley-VCH.*

pristine and doped states. Additionally, doping-induced charge-transfer complexes, which are energetically located below the neutral band, were observed for the doped unmodified D–A copolymer (Figure 5b). The charge transport through these complexes resulted in a positive Seebeck coefficient in this n-doped system. Tailoring the DOS of a doped film toward reducing those complexes' states within the bandgap led to an electrical conductivity of 1.8 S cm^{-1} and power factor of 4.5 ± 0.2 μW m^{-1} K^{-2} (Figure 5c). In a similar sense, the sign switching of the Seebeck coefficient for p-doped D–A conjugated polymers by increasing the doping level has been reported very recently.[80] These studies clearly indicate that the DOS of n-type OTEs can be tailored by molecular design, facilitating a new direction for boosting the TE performance.

Molecular packing into charge-transport pathway

The charge transport of pristine OSCs is interpreted as the percolation of free charge carriers within ordered domains through disordered regions,[81,82] which is often characterized by the field-effect mobility. As most insights into designing the OTEs were inherited from those studies related to pristine organic films, high field-effect mobility becomes an important parameter to evaluate OTEs at the early stage.[7,83] Wang et al.[46] have reported new conjugated polymers with the backbone consisting of naphtho [2,3-b:6,7-b′]dithiophenediimide (NDTI) and benzo[1,2-c:4,5-c′]- bis[1,2,5]thiadiazole (BBT) units with different side chains for n-type organic TEs. By varying solubilizing alkyl groups from 2-decyltetradecyl to 3-decylpentadecyl, the electron mobility in the transistor devices with the pristine polymer thin films was increased from 0.096 to 0.31 cm^2 V^{-1} s^{-1} because of the improved crystalline nature of the molecular packing. Thus, the electrical conductivity and power factor of the doped thins films were drastically changed from 0.18 S cm^{-1} and 0.6 μW m^{-1} K^{-2} to 5.0 S cm^{-1} and 14 μW m^{-1} K^{-2}, respectively.

However, the bulk charge mobility rather than field-effect mobility is the accurate parameter to evaluate the charge transport of a doped film because the performance of OTEs is based on the properties of the doped state. The bulk charge mobility not only depends on the packing of the organic host molecules but also on the structure changes induced by doping. This point is evidenced by some n-type D–A conjugated polymers with

DOI: 10.31635/ccschem.021.202101167
Citation: *CCS Chem.* **2021**, 3, 2702–2716
Citation denotes calendar and volume year of first online publication.
Issue Assignment: Volume 3 (2021), Issue 10

the best field-effect mobilities, but the electrical conductivities are low upon molecular doping. Huang et al.[29] have reported dihydropyrrolo[3,4-c]pyrrole-1,4-diylidenebis(thieno[3,2-b]thiophene) derivatives with aromatic and quinoid structures as the n-type TE host (Figure 6a). Both conjugated molecules have very high and comparable field-effect mobilities, however, they show very different electrical conductivities and power factors with a distinct factor of 50. The aromatic compound does not show obvious change in the intermolecular stacking upon doping, whereas the quinoid compound exhibits significantly reduced molecular packing order after molecular doping. The better tolerance of the packing order to the doping of the aromatic structure has led to much better TE performance with a figure of merit of zT = 0.23.

It is well established that "edge-on" orientation of a conjugated polymer is most favorable for the in-plane charge transport within organic field-effect transistor devices. However, a couple of recent studies indicate a mixture of "edge-on" and "face-on" orientations could accommodate the dopant molecules much better, enabling an improved host–dopant miscibility and charge-transport pathway.[28,40] For example, Wang et al.[28] designed and synthesized a series of new n-type copolymers composed of NDTI and BTI units through direct arylation polymerization. The backbone orientation was found to play an important role in dictating the electrical conductivity and the TE performance. The conjugated polymer characterized by the bimodal orientation with face- and edge-on fractions exhibited an excellent electrical conductivity of up to 11.6 S cm^{-1} and a power factor of up to 53.4 μW m^{-1} K^{-2}. They attributed the bimodal orientation to the formation of 3D conduction channels and the better accommodation of dopants, which lead to the increased doping efficiency and improved charge-transport pathway. In contrast, Koster and co-workers[30] have reported that the long-range packing order and high doping efficiency can be realized by using "arm-shaped" double-triethylene-glycol-type side chains for a fullerene derivative (Figure 6b). Upon thermal annealing, the interaction between the adjacent

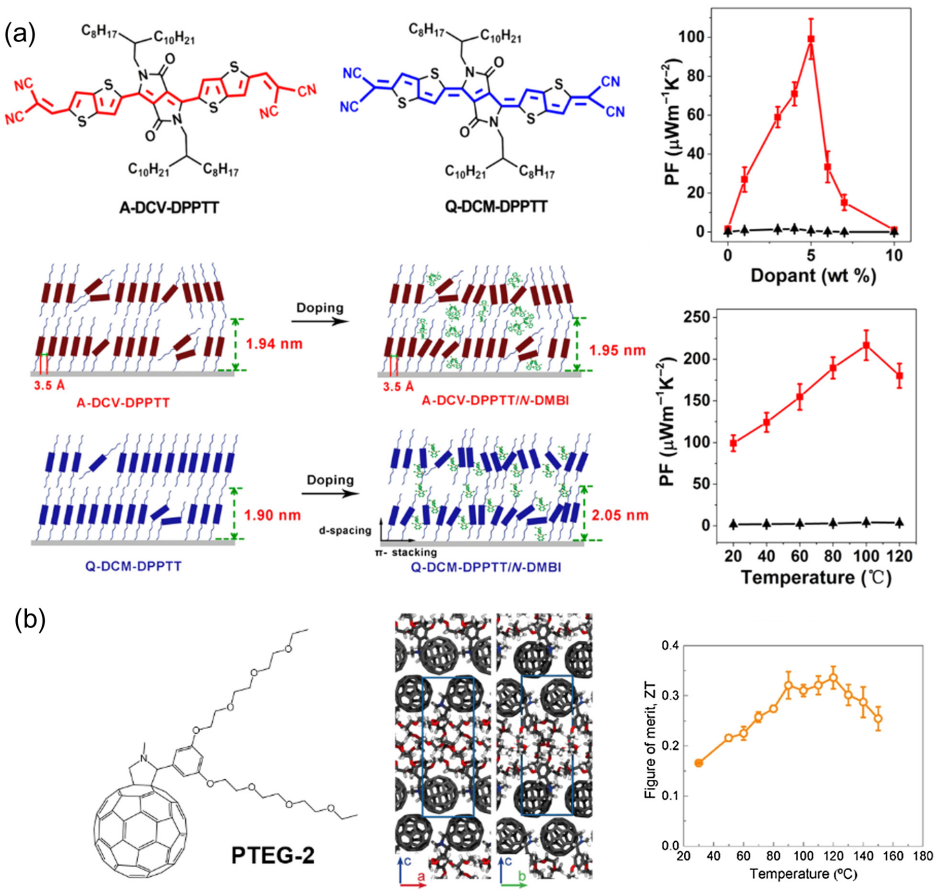

Figure 6 | *(a) Chemical structures, molecular packing and thermoelectric performance of doped A-DCV-DPPTT and Q-DCM-DPPTT. (b) Chemical structure of PTEG-1, simulated molecular packing, and figure of merit at various temperatures of molecularly doped PTEG-2 film. Reprinted with permission from the ref 29. Copyright 2017 American Chemistry Society, and the ref 30. Copyright 2020 Springer Nature.*

DOI: 10.31635/ccschem.021.202101167
Citation: *CCS Chem.* **2021**, 3, 2702–2716
Citation denotes calendar and volume year of first online publication.
Issue Assignment: Volume 3 (2021), Issue 10

polar side chains allows for a structural transition from amorphous packing to layered and ordered packing, and importantly the dopant molecules are mainly incorporated in the polar phase and the charge transport occurs in the plane of the buckyballs. As a result, a high bulk mobility of >1 $cm^2\ V^{-1}\ S^{-1}$ and doping efficiency of approximately 60% have been achieved, resulting in a record high zT = 0.34 at 120 °C. All in all, these recent studies highlight the significant impact of the packing configuration of the host and dopant molecules on the conductivity and TE performance.

Challenges and Perspective

Although significant progress has been made for n-type OTEs, many remaining challenges must be overcome to further boost the TE performance in terms of practical applications.

First, the doping efficiency in n-type OTEs is still far less than 100%, which limits the electrical conductivities to <100 S cm^{-1}, much lower than those achieved in p-doped organic films.[84] Kiefer et al.[60] reported double p-doping of conjugated polymers with a doping efficiency beyond 100%. The same strategy has not been applied for the n-doping scenario yet. More attention should be paid to develop advanced n-type dopants with favorable energy level, excellent miscibility with the organic host, and strong screening of counterions. In contrast, the mechanism of the n-doping process is still unclear, and more research efforts should be devoted toward this direction to realize precise control of the doping process.

Second, bulk electron mobilities of n-doped OSCs are typically less than 0.1 $cm^2\ V^{-1}\ s^{-1}$, which are underoptimized given the high field-effect mobilities of more than 1 $cm^2\ V^{-1}\ s^{-1}$.[85] The future n-type OTEs should be able to not only achieve the desired multiscale microstructures from the planar backbone, favorable orientation pattern, and long-range packing order but also wisely deal with the introduced dopant molecules. At the same time, how the molecular structure influences the DOS should be further studied to maximize the entropy transport per charge carrier for a given doping level.

Third, the stability of n-doped OTEs under thermal stress and ambient conditions remains a problem, limiting the practical applications. There are several reports that polar side chains could enhance the binding between host and dopant molecules, and, thus, increase the thermal stability of doped systems.[30,34,86] Nevertheless, the completely stable n-type OTEs at a temperature of over 150 °C are yet to be achieved so far. Additionally, previous studies indicate that the deep LUMO level of the host molecules and the encapsulating effect resulting from the close backbone packing or oxygen-rich side chains could help improve the air stability.[40,58,87–90] In particular, Zhu and co-workers reported quinoidal oligothiophene derivatives (QOTs) with incipient diradical character and a deep LUMO energy level (approximately −4.7 eV) to achieve excellent stability of n-type doping.[91,92] They reported the design and synthesis of unconventional n-type OTE materials based on the diradicaloids 2DQQT-S and 2DQQT-Se, which are proved to be neutral single-component organic conductors that exhibit an unprecedented air stability. Without external n-doping, a pristine film of 2DQQT-Se shows an electrical conductivity as high as 0.29 S cm^{-1} delivering a power factor of 1.4 mW $m^{-1}\ K^{-2}$.[91] Under ambient conditions, no decay in electrical conductivity is observed for over 260 h. The same group further modified the chemical structure of 2DQQT-S by increasing the number of thienoquinoidal rings, and synthesized 2DQQT. Upon doping by *N*-DMBI, the doped 2DQQT film shows a very high electrical conductivity of 14 S cm^{-1}, which could keep 80% of the initial value after storage in ambient for 240 h.[93] Guo and co-workers[31] reported two organic diradicaloids based on QOT with high stability and conductivity by employing imide-bridged fused molecular frameworks. The attachment of a strong electron-withdrawing imide group to the tetracyano-capped QOT backbones enables extremely deeply aligned LUMO levels (from −4.58 to −4.69 eV), cross-conjugated diradical characters, and remarkable ambient stabilities of the diradicaloids with half-lives >60 days. Specifically, without using any dopants, QTICN thin film exhibits a high electrical conductivity of 0.34 S cm^{-1} and a promising power factor of 1.52 μW $m^{-1}\ K^{-2}$. Future research work should further these directions to realize both completely stable and high-performance n-type OTEs.

Conclusion

In this mini review, we overviewed the emerging insights into the molecular design of n-type OTEs. The corresponding strategies to address each elementary step of the TE process have been discussed in detail. They are categorized into four sections including modulation of host–dopant miscibility, planarization of backbone, the control of electrostatics from counterions, and energetic and spatial landscape of charge transport. Due to these new strategies, huge progress for n-type OTEs has been achieved. The remaining challenges and an outlook of future research in this research direction have also been discussed. We believe that the deep understanding of the structure–property–performance relationship will provide useful guidelines to the rational design of high-performance n-type OTEs for the promising future OTE technology.

DOI: 10.31635/ccschem.021.202101167
Citation: *CCS Chem.* **2021**, 3, 2702–2716
Citation denotes calendar and volume year of first online publication.
Issue Assignment: Volume 3 (2021), Issue 10

Conflict of Interest

There is no conflict of interest to report.

References

1. Inganäs, O. Hybrid Electronics and Electrochemistry with Conjugated Polymers. *Chem. Soc. Rev.* **2010**, *39*, 2633.
2. AlSalhi, M. S.; Alam, J.; Dass, L. A.; Raja, M. Recent Advances in Conjugated Polymers for Light Emitting Devices. *Int. J. Mol. Sci.* **2011**, *12*, 2036.
3. Yang, J.; Zhao, Z.; Wang, S.; Guo, Y.; Liu, Y. Insight into High-Performance Conjugated Polymers for Organic Field-Effect Transistors. *Chem* **2018**, *4*, 2748–2785.
4. Sirringhaus, H.; Wilson, R. J.; Friend, R. H.; Inbasekaran, M.; Wu, W.; Woo, E. P.; Grell, M.; Bradley, D. D. C. Mobility Enhancement in Conjugated Polymer Field-Effect Transistors through Chain Alignment in a Liquid-Crystalline Phase. *Appl. Phys. Lett.* **2000**, *77*, 406–408.
5. Ostroverkhova, O. Organic Optoelectronic Materials: Mechanisms and Applications. *Chem. Rev.* **2016**, *116*, 13279–13412.
6. Liu, J.; Zeng, S.; Zhang, Z.; Peng, J.; Liang, Q. Optimizing the Phase-Separated Domain Size of the Active Layer via Sequential Crystallization in All-Polymer Solar Cells. *J. Phys. Chem. Lett.* **2020**, *11*, 2314–2321.
7. Venkateshvaran, D.; Broch, K.; Warwick, C. N.; Sirringhaus, H. Thermoelectric Transport Properties of High Mobility Organic Semiconductors. *Proc. SPIE* **2016**, *9943*, 10.
8. Guo, X.; Facchetti, A. The Journey of Conducting Polymers from Discovery to Application. *Nat. Mater.* **2020**, *19*, 922–928.
9. Culebras, M.; Gómez, C.; Cantarero, A. Review on Polymers for Thermoelectric Applications. *Materials (Basel)* **2014**, *7*, 6701–6732.
10. Russ, B.; Glaudell, A.; Urban, J. J.; Chabinyc, M. L.; Segalman, R. A. Organic Thermoelectric Materials for Energy Harvesting and Temperature Control. *Nat. Rev. Mater.* **2016**, *1*, 16050.
11. Kroon, R.; Mengistie, D. A.; Kiefer, D.; Hynynen, J.; Ryan, J. D.; Yu, L.; Müller, C. Thermoelectric Plastics: From Design to Synthesis, Processing and Structure-Property Relationships. *Chem. Soc. Rev.* **2016**, *45*, 6147–6164.
12. Wang, X.; Parrish, K. D.; Malen, J. A.; Chan, P. K. L. Modifying the Thermal Conductivity of Small Molecule Organic Semiconductor Thin Films with Metal Nanoparticles. *Sci. Rep.* **2015**, *5*, 16095.
13. Bubnova, O.; Khan, Z. U.; Wang, H.; Braun, S.; Evans, D. R.; Fabretto, M.; Hojati-Talemi, P.; Dagnelund, D.; Arlin, J.; Geerts, Y. H.; Desbief, S.; Breiby, D. W.; Andreasen, J. W.; Lazzaroni, R.; Chen, W. M.; Zozoulenko, I.; Fahlman, M.; Murphy, P. J.; Berggren, M.; Crispin, X. Semi-Metallic Polymers. *Nat. Mater.* **2013**, *13*, 190–194.
14. Bubnova, O.; Khan, Z. U.; Malti, A.; Braun, S.; Fahlman, M.; Berggren, M.; Crispin, X. Optimization of the Thermoelectric Figure of Merit in the Conducting Polymer Poly(3,4-Ethylenedioxythiophene). *Nat. Mater.* **2011**, *10*, 429–433.
15. Zhang, B.; Sun, J.; Katz, H. E.; Fang, F.; Opila, R. L. Promising Thermoelectric Properties of Commercial PEDOT:PSS Materials and Their Bi_2Te_3 Powder Composites. *ACS Appl. Mater. Interfaces* **2010**, *2*, 3170–3178.
16. Kim, G.-H.; Shao, L.; Zhang, K.; Pipe, K. P. Engineered Doping of Organic Semiconductors for Enhanced Thermoelectric Efficiency. *Nat. Mater.* **2013**, *12*, 719–723.
17. Vijayakumar, V.; Zhong, Y.; Untilova, V.; Bahri, M.; Herrmann, L.; Biniek, L.; Leclerc, N.; Brinkmann, M. Bringing Conducting Polymers to High Order: Toward Conductivities beyond 10^5 S Cm^{-1} and Thermoelectric Power Factors of 2 MW M^{-1} K^{-2}. *Adv. Energy Mater.* **2019**, *9*, 1–12.
18. Bell, L. E. Cooling, Heating, Generating Power, and Recovering Waste Heat with Thermoelectric Systems. *Science* **2008**, *321*, 1457–1461.
19. Schlitz, R. A.; Brunetti, F. G.; Glaudell, A. M.; Miller, P. L.; Brady, M. A.; Takacs, C. J.; Hawker, C. J.; Chabinyc, M. L. Solubility-Limited Extrinsic n-Type Doping of a High Electron Mobility Polymer for Thermoelectric Applications. *Adv. Mater.* **2014**, *26*, 2825–2830.
20. Lu, Y.; Wang, J.-Y.; Pei, J. Strategies to Enhance the Conductivity of n-Type Polymer Thermoelectric Materials. *Chem. Mater.* **2019**, *31*, 6412–6423.
21. Liu, J.; Qiu, L.; Alessandri, R.; Qiu, X.; Portale, G.; Dong, J.; Talsma, W.; Ye, G.; Sengrian, A. A.; Souza, P. C. T.; Loi, M. A.; Chiechi, R. C.; Marrink, S. J.; Hummelen, J. C.; Koster, L. J. A. Enhancing Molecular N-Type Doping of Donor-Acceptor Copolymers by Tailoring Side Chains. *Adv. Mater.* **2018**, *30*, 1704630.
22. Wang, S.; Sun, H.; Ail, U.; Vagin, M.; Persson, P. O. Å.; Andreasen, J. W.; Thiel, W.; Berggren, M.; Crispin, X.; Fazzi, D.; Fabiano, S. Thermoelectric Properties of Solution-Processed n-Doped Ladder-Type Conducting Polymers. *Adv. Mater.* **2016**, *28*, 10764–10771.
23. Huang, D.; Yao, H.; Cui, Y.; Zou, Y.; Zhang, F.; Wang, C.; Shen, H.; Jin, W.; Zhu, J.; Diao, Y.; Xu, W.; Di, C.; Zhu, D. Conjugated-Backbone Effect of Organic Small Molecules for n-Type Thermoelectric Materials with ZT over 0.2. *J. Am. Chem. Soc.* **2017**, *139*, 13013–13023.
24. Liu, J.; Qiu, L.; Portale, G.; Koopmans, M.; ten Brink, G.; Hummelen, J. C.; Koster, L. J. A. N-Type Organic Thermoelectrics: Improved Power Factor by Tailoring Host-Dopant Miscibility. *Adv. Mater.* **2017**, *29*, 1701641.
25. Liu, J.; Ye, G.; van der Zee, B.; Dong, J.; Qiu, X.; Liu, Y.; Portale, G.; Chiechi, R. C.; Koster, L. J. A. N-Type Organic Thermoelectrics of Donor-Acceptor Copolymers: Improved Power Factor by Molecular Tailoring of the Density of States. *Adv. Mater.* **2018**, *30*, 1804290.
26. Shi, K.; Zhang, F.; Di, C.-A.; Yan, T.-W.; Zou, Y.; Zhou, X.; Zhu, D.; Wang, J.-Y.; Pei, J. Toward High Performance N-Type Thermoelectric Materials by Rational Modification of BDPPV Backbones. *J. Am. Chem. Soc.* **2015**, *137*, 6979–6982.
27. Lu, Y.; Yu, Z.-D.; Un, H. I.; Yao, Z. F.; You, H. Y.; Jin, W.; Li, L.; Wang, Z. Y.; Dong, B. W.; Barlow, S.; Longhi, E.; Di, C.-a.; Zhu, D.; Wang, J. Y.; Silva, C.; Marder, S. R.; Pei, J. Persistent

DOI: 10.31635/ccschem.021.202101167
Citation: *CCS Chem.* **2021**, 3, 2702–2716
Citation denotes calendar and volume year of first online publication.
Issue Assignment: Volume 3 (2021), Issue 10

Conjugated Backbone and Disordered Lamellar Packing Impart Polymers with Efficient N-Doping and High Conductivities. *Adv. Mater.* **2021**, *33*, 1–7.
28. Wang, Y.; Takimiya, K. Naphthodithiophenediimide-Bithiopheneimide Copolymers for High-Performance n-Type Organic Thermoelectrics: Significant Impact of Backbone Orientation on Conductivity and Thermoelectric Performance. *Adv. Mater.* **2020**, *2002060*, e2002060.
29. Huang, D.; Yao, H.; Cui, Y.; Zou, Y.; Zhang, F.; Wang, C.; Shen, H.; Jin, W.; Zhu, J.; Diao, Y.; Xu, W.; Di, C. A.; Zhu, D. Conjugated-Backbone Effect of Organic Small Molecules for n-Type Thermoelectric Materials with ZT over 0.2. *J. Am. Chem. Soc.* **2017**, *139*, 13013–13023.
30. Liu, J.; van der Zee, B.; Alessandri, R.; Sami, S.; Dong, J.; Nugraha, M. I.; Barker, A. J.; Rousseva, S.; Qiu, L.; Qiu, X.; Klasen, N.; Chiechi, R. C.; Baran, D.; Caironi, M.; Anthopoulos, T. D.; Portale, G.; Havenith, R. W. A.; Marrink, S. J.; Hummelen, J. C.; Koster, L. J. A. N-Type Organic Thermoelectrics: Demonstration of ZT > 0.3. *Nat. Commun.* **2020**, *11*, 5694.
31. Yang, K.; Zhang, X.; Harbuzaru, A.; Wang, L.; Wang, Y.; Koh, C.; Guo, H.; Shi, Y.; Chen, J.; Sun, H.; Feng, K.; Ruiz Delgado, M. C.; Woo, H. Y.; Ortiz, R. P.; Guo, X. Stable Organic Diradicals Based on Fused Quinoidal Oligothiophene Imides with High Electrical Conductivity. *J. Am. Chem. Soc.* **2020**, *142*, 4329–4340.
32. Jin, K.; Hao, F.; Ding, L. Solution-Processable n-Type Organic Thermoelectric Materials. *Sci. Bull.* **2020**, *65*, 1862–1864.
33. Yuan, D.; Huang, D.; Zhang, C.; Zou, Y.; Di, C. A.; Zhu, X.; Zhu, D. Efficient Solution-Processed n-Type Small-Molecule Thermoelectric Materials Achieved by Precisely Regulating Energy Level of Organic Dopants. *ACS Appl. Mater. Interfaces* **2017**, *9*, 28795–28801.
34. Tam, T. L. D.; Xu, J. Strategies and Concepts in N-Doped Conjugated Polymer Thermoelectrics. *J. Mater. Chem. A* **2021**, *9*, 5149–5163.
35. Meng, B.; Liu, J.; Wang, L. Recent Development of N-Type Thermoelectric Materials Based on Conjugated Polymers. *Nano Mater. Sci.* **2021**, *3*, 113–123.
36. Sun, Y.; Di, C. A.; Xu, W.; Zhu, D. Advances in N-Type Organic Thermoelectric Materials and Devices. *Adv. Electron. Mater.* **2019**, *5*, 1–27.
37. Salzmann, I.; Heimel, G.; Duhm, S.; Oehzelt, M.; Pingel, P.; George, B. M.; Schnegg, A.; Lips, K.; Blum, R.-P.; Vollmer, A.; Koch, N. Intermolecular Hybridization Governs Molecular Electrical Doping. *Phys. Rev. Lett.* **2012**, *108*, 035502.
38. Lüssem, B.; Riede, M.; Leo, K. Doping of Organic Semiconductors. *Phys. Status Solidi* **2013**, *210*, 9–43.
39. Méndez, H.; Heimel, G.; Winkler, S.; Frisch, J.; Opitz, A.; Sauer, K.; Wegner, B.; Oehzelt, M.; Röthel, C.; Duhm, S.; Többens, D.; Koch, N.; Salzmann, I. Charge-Transfer Crystallites as Molecular Electrical Dopants. *Nat. Commun.* **2015**, *6*, 8560.
40. Yang, C.-Y.; Jin, W.-L.; Wang, J.; Ding, Y.-F.; Nong, S.; Shi, K.; Lu, Y.; Dai, Y.-Z.; Zhuang, F.-D.; Lei, T.; Di, C.-A.; Zhu, D.; Wang, J.-Y.; Pei, J. Enhancing the N-Type Conductivity and Thermoelectric Performance of Donor–Acceptor Copolymers through Donor Engineering. *Adv. Mater.* **2018**, *30*, 1802850.
41. Shin, Y. H.; Komber, H.; Caiola, D.; Cassinelli, M.; Sun, H.; Stegerer, D.; Schreiter, M.; Horatz, K.; Lissel, F.; Jiao, X.; McNeill, C. R.; Cimò, S.; Bertarelli, C.; Fabiano, S.; Caironi, M.; Sommer, M. Synthesis and Aggregation Behavior of a Glycolated Naphthalene Diimide Bithiophene Copolymer for Application in Low-Level n-Doped Organic Thermoelectrics. *Macromolecules* **2020**, *53*, 5158–5168.
42. Kiefer, D.; Giovannitti, A.; Sun, H.; Biskup, T.; Hofmann, A.; Koopmans, M.; Cendra, C.; Weber, S.; Anton Koster, L. J.; Olsson, E.; Rivnay, J.; Fabiano, S.; McCulloch, I.; Müller, C. Enhanced N-Doping Efficiency of a Naphthalenediimide-Based Copolymer through Polar Side Chains for Organic Thermoelectrics. *ACS Energy Lett.* **2018**, *3*, 278–285.
43. Qiu, L.; Liu, J.; Alessandri, R.; Qiu, X.; Koopmans, M.; Havenith, R. W. A.; Marrink, S. J.; Chiechi, R. C.; Anton Koster, L. J.; Hummelen, J. C. Enhancing Doping Efficiency by Improving Host-Dopant Miscibility for Fullerene-Based n-Type Thermoelectrics. *J. Mater. Chem. A* **2017**, *5*, 21234–21241.
44. Perry, E. E.; Chiu, C.-Y.; Moudgil, K.; Schlitz, R. A.; Takacs, C. J.; O'Hara, K. A.; Labram, J. G.; Glaudell, A. M.; Sherman, J. B.; Barlow, S.; Hawker, C. J.; Marder, S. R.; Chabinyc, M. L. High Conductivity in a Nonplanar N-Doped Ambipolar Semiconducting Polymer. *Chem. Mater.* **2017**, *29*, 9742–9750.
45. Shin, Y.; Massetti, M.; Komber, H.; Biskup, T.; Nava, D.; Lanzani, G.; Caironi, M.; Sommer, M. Improving Miscibility of a Naphthalene Diimide-Bithiophene Copolymer with n-Type Dopants through the Incorporation of "Kinked" Monomers. *Adv. Electron. Mater.* **2018**, *4*, 1700581.
46. Wang, Y.; Nakano, M.; Michinobu, T.; Kiyota, Y.; Mori, T.; Takimiya, K. Naphthodithiophenediimide–Benzobisthiadiazole-Based Polymers: Versatile n-Type Materials for Field-Effect Transistors and Thermoelectric Devices. *Macromolecules* **2017**, *50*, 857–864.
47. Liu, J.; Shi, Y.; Dong, J.; Nugraha, M. I.; Qiu, X.; Su, M.; Chiechi, R. C.; Baran, D.; Portale, G.; Guo, X.; Koster, L. J. A. Overcoming Coulomb Interaction Improves Free-Charge Generation and Thermoelectric Properties for n-Doped Conjugated Polymers. *ACS Energy Lett.* **2019**, *4*, 1556–1564.
48. Naab, B. D.; Gu, X.; Kurosawa, T.; To, J. W. F.; Salleo, A.; Bao, Z. Role of Polymer Structure on the Conductivity of N-Doped Polymers. *Adv. Electron. Mater.* **2016**, *2*, 1600004.
49. Deng, Y.; Chen, Y.; Zhang, X.; Tian, H.; Bao, C.; Yan, D.; Geng, Y.; Wang, F. Donor–Acceptor Conjugated Polymers with Dithienocarbazoles as Donor Units: Effect of Structure on Semiconducting Properties. *Macromolecules* **2012**, *45*, 8621–8627.
50. Deng, Y.; Liu, J.; Wang, J.; Liu, L.; Li, W.; Tian, H.; Zhang, X.; Xie, Z.; Geng, Y.; Wang, F. Dithienocarbazole and Isoindigo Based Amorphous Low Bandgap Conjugated Polymers for Efficient Polymer Solar Cells. *Adv. Mater.* **2014**, *26*, 471–476.
51. Li, Y. Molecular Design of Photovoltaic Materials for Polymer Solar Cells: Toward Suitable Electronic Energy

DOI: 10.31635/ccschem.021.202101167
Citation: *CCS Chem.* **2021**, 3, 2702–2716
Citation denotes calendar and volume year of first online publication.
Issue Assignment: Volume 3 (2021), Issue 10

Levels and Broad Absorption. *Acc. Chem. Res.* **2012**, *45*, 723–733.
52. Yan, H.; Chen, Z.; Zheng, Y.; Newman, C.; Quinn, J. R.; Dötz, F.; Kastler, M.; Facchetti, A. A High-Mobility Electron-Transporting Polymer for Printed Transistors. *Nature* **2009**, *457*, 679–686.
53. Tsao, H. N.; Cho, D. M.; Park, I.; Hansen, M. R.; Mavrinskiy, A.; Yoon, D. Y.; Graf, R.; Pisula, W.; Spiess, H. W.; Müllen, K. Ultrahigh Mobility in Polymer Field-Effect Transistors by Design. *J. Am. Chem. Soc.* **2011**, *133*, 2605–2612.
54. Estrada, L. A.; Liu, D. Y.; Salazar, D. H.; Dyer, A. L.; Reynolds, J. R. Poly[Bis-EDOT-Isoindigo]: An Electroactive Polymer Applied to Electrochemical Supercapacitors. *Macromolecules* **2012**, *45*, 8211–8220.
55. Steyrleuthner, R.; Schubert, M.; Howard, I.; Klaumünzer, B.; Schilling, K.; Chen, Z.; Saalfrank, P.; Laquai, F.; Facchetti, A.; Neher, D. Aggregation in a High-Mobility n-Type Low-Bandgap Copolymer with Implications on Semicrystalline Morphology. *J. Am. Chem. Soc.* **2012**, *134*, 18303–18317.
56. Fazzi, D.; Caironi, M.; Castiglioni, C. Quantum-Chemical Insights into the Prediction of Charge Transport Parameters for a Naphthalenetetracarboxydiimide-Based Copolymer with Enhanced Electron Mobility. *J. Am. Chem. Soc.* **2011**, *133*, 19056–19059.
57. Wang, S.; Sun, H.; Erdmann, T.; Wang, G.; Fazzi, D.; Lappan, U.; Puttisong, Y.; Chen, Z.; Berggren, M.; Crispin, X.; Kiriy, A.; Voit, B.; Marks, T. J.; Fabiano, S.; Facchetti, A. A Chemically Doped Naphthalenediimide-Bithiazole Polymer for n-Type Organic Thermoelectrics. *Adv. Mater.* **2018**, *30*, 1801898.
58. Lu, Y.; Yu, Z.; Zhang, R.; Yao, Z.; You, H.; Jiang, L.; Un, H.; Dong, B.; Xiong, M.; Wang, J.; Pei, J. Rigid Coplanar Polymers for Stable N-Type Polymer Thermoelectrics. *Angew. Chemie* **2019**, *610065*, 11512–11516.
59. Yan, X.; Xiong, M.; Li, J.-T.; Zhang, S.; Ahmad, Z.; Lu, Y.; Wang, Z.-Y.; Yao, Z.-F.; Wang, J.-Y.; Gu, X.; Lei, T. Pyrazine-Flanked Diketopyrrolopyrrole (DPP): A New Polymer Building Block for High-Performance n-Type Organic Thermoelectrics. *J. Am. Chem. Soc.* **2019**, *141*, 20215–20221.
60. Kiefer, D.; Kroon, R.; Hofmann, A. I.; Sun, H.; Liu, X.; Giovannitti, A.; Stegerer, D.; Cano, A.; Hynynen, J.; Yu, L.; Zhang, Y.; Nai, D.; Harrelson, T. F.; Sommer, M.; Moulé, A. J.; Kemerink, M.; Marder, S. R.; McCulloch, I.; Fahlman, M.; Fabiano, S.; Müller, C. Double Doping of Conjugated Polymers with Monomer Molecular Dopants. *Nat. Mater.* **2019**, *18*, 149–155.
61. Torabi, S.; Jahani, F.; Van Severen, I.; Kanimozhi, C.; Patil, S.; Havenith, R. W. A.; Chiechi, R. C.; Lutsen, L.; Vanderzande, D. J. M.; Cleij, T. J.; Hummelen, J. C.; Koster, L. J. A. Strategy for Enhancing the Dielectric Constant of Organic Semiconductors without Sacrificing Charge Carrier Mobility and Solubility. *Adv. Funct. Mater.* **2015**, *25*, 150–157.
62. Tietze, M. L.; Benduhn, J.; Pahner, P.; Nell, B.; Schwarze, M.; Kleemann, H.; Krammer, M.; Zojer, K.; Vandewal, K.; Leo, K. Elementary Steps in Electrical Doping of Organic Semiconductors. *Nat. Commun.* **2018**, *9*, 1182.
63. Burke, J. H.; Bird, M. J. Energetics and Escape of Interchain-Delocalized Ion Pairs in Nonpolar Media. *Adv. Mater.* **2019**, *31*, 1806863.
64. Aubry, T. J.; Axtell, J. C.; Basile, V. M.; Winchell, K. J.; Lindemuth, J. R.; Porter, T. M.; Liu, J. Y.; Alexandrova, A. N.; Kubiak, C. P.; Tolbert, S. H.; Spokoyny, A. M.; Schwartz, B. J. Dodecaborane-Based Dopants Designed to Shield Anion Electrostatics Lead to Increased Carrier Mobility in a Doped Conjugated Polymer. *Adv. Mater.* **2019**, *31*, 1–8.
65. Aubry, T. J.; Winchell, K. J.; Salamat, C. Z.; Basile, V. M.; Lindemuth, J. R.; Stauber, J. M.; Axtell, J. C.; Kubena, R. M.; Phan, M. D.; Bird, M. J.; Spokoyny, A. M.; Tolbert, S. H.; Schwartz, B. J. Tunable Dopants with Intrinsic Counterion Separation Reveal the Effects of Electron Affinity on Dopant Intercalation and Free Carrier Production in Sequentially Doped Conjugated Polymer Films. *Adv. Funct. Mater.* **2020**, *30*, 2001800.
66. Liu, J.; Maity, S.; Roosloot, N.; Qiu, X.; Qiu, L.; Chiechi, R. C.; Hummelen, J. C.; von Hauff, E.; Koster, L. J. A. The Effect of Electrostatic Interaction on N-Type Doping Efficiency of Fullerene Derivatives. *Adv. Electron. Mater.* **2019**, *5*, 1800959.
67. Koopmans, M.; Leiviskä, M. A. T.; Liu, J.; Dong, J.; Qiu, L.; Hummelen, J. C.; Portale, G.; Heiber, M. C.; Koster, L. J. A. Electrical Conductivity of Doped Organic Semiconductors Limited by Carrier-Carrier Interactions. *ACS Appl. Mater. Interfaces* **2020**, *12*, 56222–56230.
68. Liu, J.; Ye, G.; Potgieser, H. G. O.; Koopmans, M.; Sami, S.; Nugraha, M. I.; Villalva, D. R.; Sun, H.; Dong, J.; Yang, X.; Qiu, X.; Yao, C.; Portale, G.; Fabiano, S.; Anthopoulos, T. D.; Baran, D.; Havenith, R. W. A.; Chiechi, R. C.; Koster, L. J. A. Amphipathic Side Chain of a Conjugated Polymer Optimizes Dopant Location toward Efficient N-Type Organic Thermoelectrics. *Adv. Mater.* **2021**, *33*, 2006694.
69. Yang, C. Y.; Ding, Y. F.; Huang, D.; Wang, J.; Yao, Z. F.; Huang, C. X.; Lu, Y.; Un, H. I.; Zhuang, F. D.; Dou, J. H.; Di, C.-a; Zhu, D.; Wang, J. Y.; Lei, T.; Pei, J. A Thermally Activated and Highly Miscible Dopant for N-Type Organic Thermoelectrics. *Nat. Commun.* **2020**, *11*, 1–10.
70. Sun, Y.; Di, C.; Xu, W.; Zhu, D. Advances in N-Type Organic Thermoelectric Materials and Devices. *Adv. Electron. Mater.* **2019**, *5*, 1800825.
71. Lu, Y.; Yu, Z.-D.; Liu, Y.; Ding, Y. F.; Yang, C. Y.; Yao, Z. F.; Wang, Z. Y.; You, H. Y.; Cheng, X. F.; Tang, B.; Wang, J. Y.; Pei, J. The Critical Role of Dopant Cations in Electrical Conductivity and Thermoelectric Performance of N-Doped Polymers. *J. Am. Chem. Soc.* **2020**, *142*, 15340–15348.
72. Simonetti, O.; Giraudet, L. Transport Models in Disordered Organic Semiconductors and Their Application to the Simulation of Thin-Film Transistors. *Polym. Int.* **2019**, *68*, 620–636.
73. Arkhipov, V. I.; Heremans, P.; Emelianova, E. V.; Bässler, H. Effect of Doping on the Density-of-States Distribution and Carrier Hopping in Disordered Organic Semiconductors. *Phys. Rev. B - Condens. Matter Mater. Phys.* **2005**, *71*, 1–7.
74. Arkhipov, V. I.; Emelianova, E. V.; Heremans, P.; Bässler, H. Analytic Model of Carrier Mobility in Doped Disordered Organic Semiconductors. *Phys. Rev. B* **2005**, *72*, 235202.
75. Zuo, G.; Abdalla, H.; Kemerink, M. Impact of Doping on the Density of States and the Mobility in Organic Semiconductors. *Phys. Rev. B* **2016**, *93*, 235203.

DOI: 10.31635/ccschem.021.202101167
Citation: *CCS Chem.* **2021**, 3, 2702–2716
Citation denotes calendar and volume year of first online publication.
Issue Assignment: Volume 3 (2021), Issue 10

76. Schwarze, M.; Gaul, C.; Scholz, R.; Bussolotti, F.; Hofacker, A.; Schellhammer, K. S.; Nell, B.; Naab, B. D.; Bao, Z.; Spoltore, D.; Vandewal, K.; Widmer, J.; Kera, S.; Ueno, N.; Ortmann, F.; Leo, K. Molecular Parameters Responsible for Thermally Activated Transport in Doped Organic Semiconductors. *Nat. Mater.* **2019**, *18*, 242–248.
77. Mahan, G. D.; Sofo, J. O. The Best Thermoelectric. *Proc. Natl. Acad. Sci. U. S. A.* **1996**, *93*, 7436–7439.
78. Sun, J.; Yeh, M.-L.; Jung, B. J.; Zhang, B.; Feser, J.; Majumdar, A.; Katz, H. E. Simultaneous Increase in Seebeck Coefficient and Conductivity in a Doped Poly(Alkylthiophene) Blend with Defined Density of States. *Macromolecules* **2010**, *43*, 2897–2903.
79. Zuo, G.; Liu, X.; Fahlman, M.; Kemerink, M. High Seebeck Coefficient in Mixtures of Conjugated Polymers. *Adv. Funct. Mater.* **2018**, *28*, 1703280.
80. Liang, Z.; Choi, H. H.; Luo, X.; Liu, T.; Abtahi, A.; Ramasamy, U. S.; Hitron, J. A.; Baustert, K. N.; Hempel, J. L.; Boehm, A. M.; Ansary, A.; Strachan, D. R.; Mei, J.; Risko, C.; Podzorov, V.; Graham, K. R. N-Type Charge Transport in Heavily P-Doped Polymers. *Nat. Mater.* **2021**, *20*, 518–524.
81. Kang, K.; Watanabe, S.; Broch, K.; Sepe, A.; Brown, A.; Nasrallah, I.; Nikolka, M.; Fei, Z.; Heeney, M.; Matsumoto, D.; Marumoto, K.; Tanaka, H.; Kuroda, S.; Sirringhaus, H. 2D Coherent Charge Transport in Highly Ordered Conducting Polymers Doped by Solid State Diffusion. *Nat. Mater.* **2016**, *15*, 896–902.
82. Noriega, R.; Rivnay, J.; Vandewal, K.; Koch, F. P. V; Stingelin, N.; Smith, P.; Toney, M. F.; Salleo, A. A General Relationship between Disorder, Aggregation and Charge Transport in Conjugated Polymers. *Nat. Mater.* **2013**, *12*, 1038–1044.
83. Zhang, F.; Di, C. Exploring Thermoelectric Materials from High Mobility Organic Semiconductors. *Chem. Mater.* **2020**, *32*, 2688–2702.
84. Yamashita, Y.; Tsurumi, J.; Ohno, M.; Fujimoto, R.; Kumagai, S.; Kurosawa, T.; Okamoto, T.; Takeya, J.; Watanabe, S. Efficient Molecular Doping of Polymeric Semiconductors Driven by Anion Exchange. *Nature* **2019**, *572*, 634–638.
85. Paterson, A. F.; Singh, S.; Fallon, K. J.; Hodsden, T.; Han, Y.; Schroeder, B. C.; Bronstein, H.; Heeney, M.; McCulloch, I.; Anthopoulos, T. D. Recent Progress in High-Mobility Organic Transistors: A Reality Check. *Adv. Mater.* **2018**, *30*, 1–33.
86. Li, J.; Rochester, C. W.; Jacobs, I. E.; Aasen, E. W.; Friedrich, S.; Stroeve, P.; Moulé, A. J. The Effect of Thermal Annealing on Dopant Site Choice in Conjugated Polymers. *Org. Electron. physics, Mater. Appl.* **2016**, *33*, 23–31.
87. de Leeuw, D. M.; Simenon, M. M. J.; Brown, A. R.; Einerhand, R. E. F. Stability of N-Type Doped Conducting Polymers and Consequences for Polymeric Microelectronic Devices. *Synth. Met.* **1997**, *87*, 53–59.
88. Nava, D.; Shin, Y.; Massetti, M.; Jiao, X.; Biskup, T.; Jagadeesh, M. S.; Calloni, A.; Duò, L.; Lanzani, G.; McNeill, C. R.; Sommer, M.; Caironi, M. Drastic Improvement of Air Stability in an N-Type Doped Naphthalene-Diimide Polymer by Thionation. *ACS Appl. Energy Mater.* **2018**, *1*, 4626–4634.
89. Liu, J.; Qiu, L.; Portale, G.; Torabi, S.; Stuart, M. C. A.; Qiu, X.; Koopmans, M.; Chiechi, R. C.; Hummelen, J. C.; Anton Koster, L. J. Side-Chain Effects on N-Type Organic Thermoelectrics: A Case Study of Fullerene Derivatives. *Nano Energy* **2018**, *52*, 183–191.
90. Feng, K.; Guo, H.; Wang, J.; Shi, Y.; Wu, Z.; Su, M.; Zhang, X.; Son, J. H.; Woo, H. Y.; Guo, X. Cyano-Functionalized Bithiophene Imide-Based n-Type Polymer Semiconductors: Synthesis, Structure–Property Correlations, and Thermoelectric Performance. *J. Am. Chem. Soc.* **2021**, *143*, 1539–1552.
91. Yuan, D.; Guo, Y.; Zeng, Y.; Fan, Q.; Wang, J.; Yi, Y.; Zhu, X. Air-Stable n-Type Thermoelectric Materials Enabled by Organic Diradicaloids. *Angew. Chemie Int. Ed.* **2019**, *58*, 4958–4962.
92. Yuan, D. Stable N-Doped Conductors Enabled by Organic Diradicals. *Chem* **2019**, *5*, 744–745.
93. Yuan, D.; Huang, D.; Rivero, S. M.; Carreras, A.; Zhang, C.; Zou, Y.; Jiao, X.; McNeill, C. R.; Zhu, X.; Di, C.-a.; Zhu, D.; Casanova, D.; Casado, J. Cholesteric Aggregation at the Quinoidal-to-Diradical Border Enabled Stable n-Doped Conductor. *Chem* **2019**, *5*, 964–976.

DOI: 10.31635/ccschem.021.202101167
Citation: *CCS Chem.* **2021**, 3, 2702–2716
Citation denotes calendar and volume year of first online publication.
Issue Assignment: Volume 3 (2021), Issue 10